

Analysis of Wave Propagation in 1D Inhomogeneous Media

Patrick Guidotti* James V. Lambers[†] Knut Solna[‡]

July 15, 2005

Abstract

In this paper we consider the one dimensional inhomogeneous wave equation with particular focus on its spectral asymptotic properties and its numerical resolution. In a first part of the paper we analyze the asymptotic nodal point distribution of high frequency eigenfunctions, which, in turn gives further information about the asymptotic behavior of eigenvalues and eigenfunctions. We then turn to the behavior of eigenfunctions in the high and low frequency limit. In the latter case we derive an homogenization limit whereas in the first we show that a sort of self-homogenization occurs at high frequencies. We also remark on the structure of the solution operator and its relation to desired properties of any numerical approximation.

We subsequently shift our focus to the latter and present a Galerkin scheme based on a spectral integral representation of the propagator in combination with Gaussian quadrature in the spectral variable with a frequency-dependent measure. The proposed scheme yields accurate resolution of both high and low frequency components of the solution and as a result proves to be more accurate than available schemes at large time steps for both smooth and non-smooth speeds of propagation.

*Department of Mathematics, University of California at Irvine, Irvine, CA 92697-3875, partially supported by NSF CMS0330470

[†]Department of Petroleum Engineering, Stanford University, Stanford, CA 94305-2220

[‡]Department of Mathematics, University of California at Irvine, Irvine, CA 92697-3875, supported by NSF DMS0112416 and DMS0307011.

1 Introduction

In this paper we consider the one dimensional inhomogeneous wave equation

$$\begin{cases} \partial_{tt}u - c^2(x)\partial_{xx}u = 0 & \text{in } (0,1) \times \mathbb{R}, \\ u + \beta\partial_xu = 0 & \text{on } \{0,1\} \times \mathbb{R}, \end{cases} \quad (1.1)$$

with $\beta = 0$ and $c \in L_\infty(0,1)$ and strictly positive. Our results remain valid for any β but, for the sake of brevity, we shall present them for the case $\beta = 0$ only. After some remarks on the structure of the solution operator and on the implications for its numerical approximability, we turn to the main focus of the paper: Spectral asymptotics and numerical resolution of (1.1).

As for the asymptotic spectral properties of the generator, the general result of [17, Theorem 1.2.1] would readily imply that

$$\lambda_k \approx \left(k\pi \left/ \int_0^1 \frac{dx}{c(x)} \right. \right)^2, \quad k \text{ large}$$

for the eigenvalues of the generator $\mathcal{A} = -c^2(x)\partial_{xx}$. In this particular case, however, led by the physical meaning of the coefficient c , we are able to obtain information about the asymptotic behavior of the nodal points of high frequency eigenfunctions and, from that, infer about their asymptotic shape. The analysis is based on a shooting method for the computation of the eigenvalue/eigenfunction pairs and the self-similar nature of the problem in combination with the use of a canonical transformation. In particular, we observe that a sort of self-homogenization occurs at high frequencies (cf. section 2.3). It turns out that the same ideas can be profitably employed to obtain homogenization results for rapidly varying coefficients. These are similar to the result derived in for instance [14] for the self-adjoint case using a variational approach. Here, however, our focus is an asymptotic approximation for the spectrum and we present the approach in section 2.4.

Then, in section 3, we integrate some of the ideas developed into a numerical approach to high order/large time step resolution of (1.1). This approach employs Krylov subspace spectral methods, first introduced in [12]. These methods are Galerkin methods in which each component of the solution in the chosen basis of trial functions is computed using an approximation of the propagator belonging to a low-dimensional Krylov subspace of the operator \mathcal{A} . Each approximation is based on the use of Gaussian quadrature to evaluate Riemann-Stieltjes integrals over the spectral domain as described in [7]. Because the Krylov subspace approximation of \mathcal{A} is

constructed using Gaussian rules that are tailored to each component, all components can be resolved more accurately than with traditional spectral methods.

Based on the encouraging results for the one dimensional case, we intend to pursue the possibility of adapting the techniques used in this paper to perform similar analysis in the higher dimensional case.

2 Analytic structure of the propagator

In this section we derive a spectral representation formula for the solution of the inhomogeneous wave equation in a bounded one dimensional interval as given in (1.1). In order to do so we need to analyze the spectral properties of non-selfadjoint boundary value problem $(\mathcal{A}, \mathcal{B})$ given by

$$\mathcal{A} = c^2(x)\partial_{xx}, \quad (2.1)$$

$$\mathcal{B} = \gamma_j, \quad j = 0, 1. \quad (2.2)$$

where γ_j denotes the trace operator at $j = 0, 1$. This is done in subsection 2.1. The analytic structure of the solution makes the relation between the conservation and reversibility properties of the equation apparent (subsection 2.2). In particular they can be concisely formulated in terms of a functional relation satisfied by the propagator (evolution operator).

2.1 Properties of the generator

We start by collecting some information about the spectral properties of the generator, that is, of the boundary value problem (2.1)-(2.2). We therefore study

$$-c^2(x)\partial_{xx}u = \lambda u, \quad (2.3)$$

$$u(j) = 0, \quad j = 0, 1. \quad (2.4)$$

Lemma 2.1 *All eigenvalues of (2.1)-(2.2) are strictly positive real and simple. The eigenfunction corresponding to the first (smallest) eigenvalue can be chosen to be positive.*

Proof Assume that $\lambda \in \mathbb{C}$ is an eigenvalue of (2.3)-(2.4) and u an associated eigenfunction, then

$$\lambda \int_0^1 \frac{|u(x)|^2}{c^2(x)} dx = \int_0^1 |\partial_x u(x)|^2 dx$$

which implies the positivity of the eigenvalue. Moreover, an eigenvalue of (2.3)-(2.4) is given when the boundary conditions are linearly dependent and therefore the kernel has always at most dimension one, which gives simplicity of the eigenvalues. Finally since the operator has empty kernel and compact resolvent, the spectrum is a pure point spectrum which concludes the proof. \square

Borrowing from the self-adjoint terminology, we call the first eigenvalue λ_1 the principal eigenvalue. Next we show that it is a strictly monotone function of the size of the domain.

Lemma 2.2 *Let $x_0 \in (0, 1)$ and $\lambda_1(x_0)$ be the principal eigenvalue for the Dirichlet problem for $-c^2(x)\partial_{xx}$ on $[0, x_0]$. Then*

$$\lambda(x_1) > \lambda(x_0), \quad 0 < x_1 < x_0 \leq 1.$$

Proof Normalizing eigenfunctions φ by the requirement

$$\partial_x \varphi(0) = 1$$

we can look for them by considering the initial value problem

$$\begin{cases} -\partial_{xx} u = \lambda \frac{u}{c^2(x)}, & x \in [0, 1], \\ u(0) = 0, \partial_x u(0) = 1. \end{cases} \quad (2.5)$$

For $\lambda = 0$ no nontrivial solution can be found, but, by increasing its magnitude the value of the solution at $x = 1$ can be reduced until it becomes zero for the first time. This gives λ_1 and $\varphi_1 \geq 0$ for $[0, 1]$. It is therefore also obvious that λ needs to be further increased to obtain a zero at $x_1 < 1$, which, in its turn, determines λ_1 and φ_1 for the interval $[0, x_1]$. \square

It turns out that we can determine all other eigenvalues and order them according to their size or equivalently according to the number of their zeros.

Lemma 2.3 *For every $n \in \mathbb{N}$ there is exactly one simple eigenvalue $\lambda_n > 0$ for the Dirichlet problem for $-c^2(x)\partial_{xx}$ on $[0, 1]$ such that the associated eigenfunction φ_n has exactly $n + 1$ zeros (counting the boundary points).*

Proof By using exactly the same arguments as in the proof of lemma 2.2 one can obtain all eigenfunctions as solutions the initial value problem (2.5) by gradually increasing λ in order to produce, one by one, new zeros in the interval $[0, 1]$. They therefore can be numbered by using their zeros. \square

Next we introduce a functional setting which allows us to obtain a spectral representation of the operator. Let $L_2(0, 1)$ be the Lebesgues space of square integrable functions. Denote by A the $L_2(0, 1)$ -realization of \mathcal{A} with domain of definition given by $\text{dom}(A) = H^2(0, 1) \cap H_0^1(0, 1)$, the space of H^2 functions which vanish on the boundary. Since A has compact resolvent, it allows for a spectral calculus.

Lemma 2.4 *The operator A can be represented by*

$$A = \sum_{n=1}^{\infty} \lambda_n \langle \varphi_n^*, \cdot \rangle \varphi_n, \quad (2.6)$$

where $(\varphi_n)_{n \in \mathbb{N}}$ and $(\varphi_n^*)_{n \in \mathbb{N}}$ are the eigenfunctions of A and A^* to the eigenvalue λ_n , respectively. Here A^* is given by the L_2 -realization of $-\partial_{xx}(c^2(x)\cdot)$ with Dirichlet boundary conditions.

Proof Since all eigenvalues are simple and $\lambda = 0$ is not one of them the operator A^{-1} does not contain any nontrivial Jordan blocks nor does it contains a quasi-nilpotent operator. It follows that the operator A allows for the claimed spectral representation. See [3] for more details. One needs only to observe that the spectral projection E_{λ_n} is given by $\langle \varphi_n^*, \cdot \rangle$, where φ_n^* can be defined through

$$\varphi_n^* \perp \overline{\text{span}}\{\varphi_k : n \neq k \in \mathbb{N}\} \text{ and } \langle \varphi_n^*, \varphi_n \rangle = 1$$

and can be easily verified to be an eigenfunction of A^* to the eigenvalue λ_n .
□

Remark 2.5 *In general, the functions $(\varphi_n)_{n \in \mathbb{N}}$ are not an orthogonal system. They are, however, asymptotically orthogonal for smooth c and almost orthogonal for small perturbations of a constant c as we shall see in the next sections. It should be observed that the operator A becomes self-adjoint with respect to the weighted scalar product*

$$(u|v) = \int_0^1 u(x)v(x)/c^2(x) dx.$$

This provides a different point of view but produces the same spectral resolution of A . See also 2.7.

2.2 Structure of the solution

The spectral representation of the generator A allows us to obtain a representation of the solution operator (propagator) in terms of the sine and cosine families generated by A by a simple functional calculus. Introduce

$$R_1(t) = A^{-1/2} \sin(t\sqrt{A}) := \sum_{n=1}^{\infty} \frac{\sin(t\sqrt{\lambda_n})}{\sqrt{\lambda_n}} \langle \varphi_n^*, \cdot \rangle \varphi_n, \quad (2.7)$$

$$R_0(t) = \cos(t\sqrt{A}) := \sum_{n=1}^{\infty} \cos(t\sqrt{\lambda_n}) \langle \varphi_n^*, \cdot \rangle \varphi_n, \quad (2.8)$$

where taking the square root of the operator poses no problem even though the operator is not self-adjoint. Then the propagator of (1.1) can be written as

$$P(t) = \begin{bmatrix} R_0(t) & R_1(t) \\ -A R_1(t) & R_0(t) \end{bmatrix}. \quad (2.9)$$

Remark 2.6 *The fact that the wave equation is reversible can be seen through the identities*

$$R_0^2(t) + A R_1^2(t) = \text{id}_{L_2(0,1)}, \quad R_0(t) R_1(t) = R_1(t) R_0(t), \quad t \in \mathbb{R} \quad (2.10)$$

which imply

$$P(t) P(-t) = P(-t) P(t) = \begin{bmatrix} \text{id}_{L_2(0,1)} & 0 \\ 0 & \text{id}_{L_2(0,1)} \end{bmatrix} \quad (2.11)$$

We observe that our ultimate goal is an efficient numerical scheme for the solution of (1.1). We are in particular interested in non dissipative and non dispersive schemes. The functional relations (2.10) make the constraints apparent which such a scheme should satisfy. Next we introduce an appropriate energy norm $\| \cdot \|_{\sqrt{A}}$ and show that it is conserved along solutions of (1.1). This is done by means of the basis development in terms of the eigenfunctions $(\varphi_n)_{n \in \mathbb{N}}$. Let $u \in L_2(0, 1)$, then we can write

$$u = \sum_{n=1}^{\infty} \underbrace{\langle \varphi_n^*, u \rangle}_{u_n} \varphi_n.$$

Then, taking $(u, v) \in H_0^1(0, 1) \times L_2(0, 1)$, we define

$$\|(u, v)\|_{\sqrt{A}} = \sqrt{\sum_{n=1}^{\infty} (\lambda_n u_n^2 + v_n^2)} \quad (2.12)$$

whenever the right-hand-side is finite.

Remark 2.7 *It is not a priori clear that (2.12) does define a norm which is equivalent to the standard norm of $H_0^1(0,1) \times L_2(0,1)$. This follows from the fact that, in the described setting, $\varphi_n^* = \varphi_n/c^2(x)$ and the fact that the speed of propagation is bounded above and below. The relation between the eigenfunctions is a manifestation of 2.5. This also means that $(\varphi_n)_{n \in \mathbb{N}}$ is a frame and $(\varphi_n^*)_{n \in \mathbb{N}}$ its dual frame. For a definition and characterization of frames we refer [2].*

Lemma 2.8 *For any solution of (1.1) with $\beta = 0$ one has*

$$\|(u(t), \dot{u}(t))\|_{\sqrt{A}} = \|(u(0), \dot{u}(0))\|_{\sqrt{A}}, \quad t \in \mathbb{R}. \quad (2.13)$$

Proof Denote the initial value $(u(0), \dot{u}(0))$ by (u^0, \dot{u}^0) . Then, by developing in the basis of eigenfunctions, we can write the solution as

$$(u(t), \dot{u}(t)) = \left(\sum_{n=1}^{\infty} \left[\cos(t\sqrt{\lambda_n})u_n^0 + \frac{1}{\sqrt{\lambda_n}} \sin(t\sqrt{\lambda_n})\dot{u}_n^0 \right] \varphi_n, \right. \\ \left. \sum_{n=1}^{\infty} \left[-\sqrt{\lambda_n} \sin(t\sqrt{\lambda_n})u_n^0 + \cos(t\sqrt{\lambda_n})\dot{u}_n^0 \right] \varphi_n \right). \quad (2.14)$$

A simple computation then shows that

$$\sum_{n=1}^{\infty} \left\{ \lambda_n \left[\cos(t\sqrt{\lambda_n})u_n^0 + \frac{1}{\sqrt{\lambda_n}} \sin(t\sqrt{\lambda_n})\dot{u}_n^0 \right]^2 \right. \\ \left. + \left[-\sqrt{\lambda_n} \sin(t\sqrt{\lambda_n})u_n^0 + \cos(t\sqrt{\lambda_n})\dot{u}_n^0 \right]^2 \right\} = \sum_{n=1}^{\infty} \lambda_n (u_n^0)^2 + (\dot{u}_n^0)^2.$$

□

2.3 High frequency spectral asymptotics

In this subsection we show that a sort of self-homogenization occurs at high frequency which makes the asymptotic behavior of the eigenvalues and eigenfunctions of A very simple. We begin with the following lemma concerning small perturbations of the constant coefficient case.

Lemma 2.9 *Assume that $c \in C^1([0,1])$ is almost constant, that is, that $\|c'\|_{\infty} \leq \varepsilon$. Then the spectrum of A is a small perturbation of that of the operator \bar{A} given by*

$$\text{dom } \bar{A} = H^2(0,1) \cap H_0^1(0,1), \quad \bar{A}u = \bar{c}^2 \partial_{xx}u, \quad u \in \text{dom}(A) \quad (2.15)$$

for $\bar{c} = \left(\int_0^1 \frac{1}{c(x)} dx \right)^{-1}$.

Proof Introducing the change of variables given by

$$y = \Phi(x) = \bar{c} \int_0^x \frac{1}{c(\xi)} d\xi \quad (2.16)$$

which leaves the interval invariant, the operator A in the new variables takes on the form

$$c^2(x)\partial_{xx} = \bar{c}^2 \partial_{yy} - \bar{c}c'(\Phi^{-1}(y))\partial_y.$$

The result then follows from the continuous dependence of the operator on its coefficient functions. \square

Remark 2.10 *It should be observed that the coefficient c can be thought of as the speed of propagation through the medium in the interval $[0, 1]$. Then the integral $\int_0^1 \frac{1}{c(x)} dx$ can be interpreted as the time it takes to go from one end to other of the medium. Thus the averaged coefficient actually measures the “effective size” of the interval.*

It turns out that this kind of averaging is always taking place regardless of the size and shape of the coefficient c , at least at high frequencies. The next proposition makes this precise and also gives an approximation for the high frequency eigenfunctions.

Proposition 2.11 *For large $n \in \mathbb{N}$ the asymptotic behavior of the eigenvalues of A is given by*

$$\lambda_n \approx \frac{(n\pi)^2}{\left(\int_0^1 \frac{1}{c(\xi)} d\xi\right)^2}. \quad (2.17)$$

Moreover, the eigenfunctions φ_n have the following asymptotic shape

$$\varphi_n(x) \approx \sin\left(\pi \frac{x - x_{j-1}}{x_j - x_{j-1}}\right), \quad x \in [x_{j-1}, x_j] \quad (2.18)$$

where $0 = x_0 < x_1 < \dots < x_n = 1$ have to be chosen such that

$$\int_{x_{j-1}}^{x_j} \frac{1}{c(\xi)} d\xi = \frac{1}{n} \int_0^1 \frac{1}{c(\xi)} d\xi, \quad j = 1, \dots, n. \quad (2.19)$$

Proof We know from lemmata 2.1-2.3 that the n -th eigenfunction φ_n has $n + 1$ zeros in $[0, 1]$. Denote them by

$$0 = x_0 < x_1 < \dots < x_n = 1.$$

If λ_n is the associated eigenvalue, then it is also the principal eigenvalue λ_n^j of the problems

$$\begin{cases} c^2(x)\partial_{xx}u = \lambda u, & \text{in } [x_{j-1}, x_j] \\ u(x_{j-1}) = u(x_j) = 0. \end{cases}$$

for $j = 1, \dots, n$. So, in particular one has $\lambda_n^j = \lambda_n$, $j = 1, \dots, n$. By blowing up the intervals $[x_{j-1}, x_j]$ to the fixed interval $[0, 1]$ by means of

$$x = x_{j-1} + y(x_j - x_{j-1}), \quad y \in [0, 1]$$

we obtain

$$\begin{cases} \frac{\tilde{c}^2(y)}{(x_j - x_{j-1})^2} \partial_{yy} \tilde{u} = \lambda \tilde{u}, & \text{in } [0, 1] \\ u(0) = u(1) = 0. \end{cases}$$

where now $\tilde{c}(y) = c(x_{j-1} + y(x_j - x_{j-1}))$ is a slowly varying coefficient provided n is large. Lemma 2.9 therefore gives

$$\lambda_n^j \approx \frac{\pi^2}{(x_j - x_{j-1})^2} \left(\frac{1}{x_j - x_{j-1}} \int_{x_{j-1}}^{x_j} \frac{1}{c(\xi)} d\xi \right)^{-2} = \frac{\pi^2}{\left(\int_{x_{j-1}}^{x_j} \frac{1}{c(\xi)} d\xi \right)^2}.$$

and subsequently that

$$\int_{x_{j-1}}^{x_j} \frac{1}{c(\xi)} d\xi = \frac{1}{n} \int_0^1 \frac{1}{c(\xi)} d\xi$$

since we know already that $\lambda_n^1 = \dots = \lambda_n^n = \lambda_n$. We conclude that the subintervals are uniquely determined. Lemma 2.15 also entails that the eigenfunctions on the subintervals all have approximately the form

$$\varphi_n^j(x) = \sin\left(\pi \frac{x - x_{j-1}}{x_j - x_{j-1}}\right), \quad x \in [x_{j-1}, x_j].$$

□

Remark 2.12 *It is interesting to observe that to first order the asymptotic behavior of the eigenvalues only contains average information concerning the coefficient whereas the asymptotic behavior of eigenfunctions reflects local averages taken at the scale determined by the number of its zeros.*

2.4 Low frequency spectral asymptotics

In this section we consider the asymptotic behavior of the low frequency part of the spectrum. We describe it in the regime where the length x_0 of the medium is large. That is, we consider the problem

$$\begin{cases} -c^2(x)\partial_{xx}u = \lambda u, & x \in [0, x_0], \\ u(0) = 0, u(x_0) = 0 \end{cases} \quad (2.20)$$

in the limit $x_0 \rightarrow \infty$. Observe that we allow for large $\mathcal{O}(1)$ fluctuations in the local speed c . If we set $\epsilon = 1/x_0$ and make the change of variables $y = \epsilon x$ this problem becomes

$$\begin{cases} -c^2\left(\frac{y}{\epsilon}\right)\partial_{yy}u^\epsilon = \frac{\lambda}{\epsilon^2}u^\epsilon = \lambda^\epsilon u^\epsilon, & y \in [0, 1], \\ u^\epsilon(0) = 0, u^\epsilon(1) = 0. \end{cases} \quad (2.21)$$

This is a homogenization scaling. The self-adjoint case when σ is periodic is discussed in [1], for instance, and the case when σ is random and varies on a microscale is discussed in [10]. Wave propagation in the quasistatic limit corresponding to a scaling of the above type is discussed in for instance [14, 15] where the group velocity in this limit is derived from the homogenized equations. Here we consider the leading part of the spectrum of the non self-adjoint problem with rapidly varying coefficients. It can be characterized by the following proposition.

Proposition 2.13 *Let $x_0 \in \mathbb{R}$ and $(\lambda_n(x_0), \varphi_n(x; x_0))$ be the n 'th pair of eigenvalue and function of the Dirichlet problem (2.20). For $f \in C^1$ assume that*

$$\int_0^y c^{-2}\left(\frac{s}{\epsilon}\right) f(s) ds = c_*^{-2} \int_0^y f(s) ds (1 + \mathcal{O}(\epsilon^p)) \quad (2.22)$$

with

$$c_*^{-2} = \lim_{\epsilon \rightarrow 0} \int_0^1 c^{-2}(s/\epsilon) ds, \quad 0 < \underline{c} < c(x) < \bar{c} < \infty, \quad p > 0.$$

Then

$$\lambda_n(x_0) \sim (n\pi)^2 c_*^2 / x_0^2 \quad (2.23)$$

$$\varphi_n(x; x_0) \sim \sqrt{\frac{2}{x_0}} \sin(n\pi x / x_0) \quad (2.24)$$

as $x_0 \rightarrow \infty$.

Proof As in the proof of Proposition 2.11 we use a shooting argument to solve the eigenvalue problem. It involves normalizing the eigenfunction by requiring $\partial_y \phi(0) = 1$ and writing (2.21) as:

$$\begin{cases} -\partial_{yy} \varphi^\epsilon = c^{-2} \left(\frac{y}{\epsilon}\right) \lambda^\epsilon \varphi^\epsilon, & y \in [0, 1], \\ \varphi^\epsilon(0) = 0, \quad \partial_y \varphi^\epsilon(0) = 1. \end{cases} \quad (2.25)$$

Again for $\lambda^\epsilon = 0$ no non-trivial solution can be found. By increasing λ^ϵ the value of φ^ϵ can be reduced until it becomes zero for the first time. This value gives the first eigenvalue λ_1^ϵ and the corresponding leading eigenfunction φ_1^ϵ . In order to describe these for x_0 large we introduce $v = (v_1, v_2)^T = (\varphi_1^\epsilon, \varphi_{1,y}^\epsilon)^T$ and obtain the initial value problem

$$v_y = \begin{bmatrix} 0 & 1 \\ -\lambda_1^\epsilon c^{-2} & 0 \end{bmatrix} v, \quad v(0) = (0, 1)^T.$$

Then, we construct an approximating sequence v^n by letting

$$v_y^0 = \begin{bmatrix} 0 & 1 \\ -\lambda_1^\epsilon c_*^{-2} & 0 \end{bmatrix} v^0,$$

and

$$v_y^n = \begin{bmatrix} 0 & 1 \\ -\lambda_1^\epsilon c^{-2} & 0 \end{bmatrix} v^{n-1}, \quad n \geq 1, \quad (2.26)$$

with $v^n(0) = (0, 1)$. The increments $\delta v^n = v^n - v^{(n-1)}$ solve the same equation (2.26) and we find

$$\|\delta v^n\|_1(y) \leq (1 + (\pi \bar{c}/\underline{c})^2) \int_0^y \|\delta v^{(n-1)}\|_1(s) ds.$$

Observe next that

$$\|\delta v^1\|_1(y) = \lambda_1^\epsilon \left\| \left[\int_0^y (c^{-2} - c_*^{-2}) v_1^0(s) ds \right] \right\|_1 < \epsilon^p c_1 y,$$

and

$$\|\delta v^n\|_1(y) \leq \epsilon^p \frac{(c_2 y)^n}{n!}, \quad n \geq 0,$$

where here and below c_j are constants independent of ϵ . Thus, v^n form a Cauchy sequence and

$$\sup_{y \in (0,1)} |v_1^0 - \varphi_1^\epsilon|(y) \leq \epsilon^p e^{c_2}.$$

We next establish that v_1^0 is close to the principal eigenfunction associated with the constant speed c_* . This follows since explicitly

$$v_1^0(y) = \frac{\sin(\sqrt{\lambda_1^\epsilon/c_*^2} y)}{\sqrt{\lambda_1^\epsilon/c_*^2}},$$

moreover, $|v_1^0(1)| \leq \epsilon^p \exp(c_2)$ and $y = 1$ is the first zero of φ^ϵ which is a positive function, thus, $\exists \epsilon_0 > 0$ such that $\forall \epsilon \leq \epsilon_0$:

$$\begin{aligned} |\lambda_1^\epsilon - (\pi c_*)^2| &\leq \epsilon^p c_3 \\ \sup_{y \in (0,1)} \left| \varphi_1^\epsilon(y) - \frac{\sin(\pi y)}{\pi} \right| &\leq \epsilon^p c_4 \end{aligned}$$

Finally, upon a normalization and a change of argument we arrive at (2.23) for $n = 1$.

Next, we consider the case with general n which follows by induction. Let φ_n^ϵ be the n 'th eigenfunction associated with (2.25) which can be constructed as above via a shooting procedure where λ^ϵ is successively increased. The eigenvalues are again identified with those values for λ^ϵ that give a new zero in the interval $[0, 1]$, since the additional zero only can enter at $y = 1$ because $\varphi_{yy}^\epsilon = 0$ only for $\varphi^\epsilon = 0$.

Now assume that (2.23) hold for the first n eigenfunctions. Then, $\exists \epsilon_0 > 0$ so that for $\epsilon \leq \epsilon_0$

$$|\partial_y \varphi_n^\epsilon(1)| > 1/2,$$

it follows that $\exists c_1(n) > 0$ such that $|\lambda_{n+1}^\epsilon - \lambda_n^\epsilon| \geq c_1(n)$. By an argument as above $\exists c_2(n)$ such that

$$\sup_{y \in (0,1)} \left| \varphi_{n+1}^\epsilon(y) - \frac{\sin(\sqrt{\lambda_{n+1}^\epsilon/c_*^2} y)}{\sqrt{\lambda_{n+1}^\epsilon/c_*^2}} \right| \leq \epsilon^p e^{c_2(n)}$$

and we find $\exists c_3(n) > 0$ such that $\sin(\sqrt{\lambda_{n+1}^\epsilon/c_*^2} y)$ has exactly $n + 2$ zeros in $[0, 1 + \epsilon^p c_3(n)]$. Now, by proceeding as above, (2.23) follows for $n + 1$ and therefore for general n . \square

Remark 2.14 *The condition (2.22) is satisfied with $p = 1$ if for instance*

$$c^{-2}(x) = c_*^{-2}(1 + \mu'(x))$$

with $\mu(x)$ being a bounded function. More generally for

$$c^{-2}(x) = c_*^{-2}(1 + \nu(x))$$

we find

$$\int_0^y c^{-2} \left(\frac{s}{\epsilon} \right) f(s) ds = c_*^{-2} \left(\int_0^y f(s) ds + \epsilon \left(Y \left(\frac{y}{\epsilon} \right) f(y) - \int_0^y Y \left(\frac{s}{\epsilon} \right) f'(s) ds \right) \right)$$

with

$$Y(x) = \int_0^x \nu(s) ds.$$

Thus, if $Y(x) = \mathcal{O}(x^{1-p})$ with $p > 0$, then (2.22) is satisfied.

3 Krylov Subspace Spectral Methods

In this section we apply Krylov subspace spectral methods developed in [12] to the problem (1.1) with $\beta = 0$ and the initial conditions

$$u(x, 0) = f(x), \quad u_t(x, 0) = g(x), \quad x \in (0, 1). \quad (3.1)$$

3.1 Symmetrization

We first apply two transformations to the differential operator $\mathcal{A} = c^2(x)\partial_{xx}$ defined in (2.1). As in previous discussion, we focus on the operator A that is the $L_2(0, 1)$ -realization of \mathcal{A} defined on $\text{dom}(A) = H^2(0, 1) \cap H_0^1(0, 1)$. First, we apply the change of variables (2.16) to obtain

$$\bar{A} = \bar{c}^2 \partial_{xx} - \bar{c} \bar{c}' (\Phi^{-1}(x)) \partial_x, \quad (3.2)$$

where, we recall,

$$\bar{c} = \left(\int_0^1 \frac{1}{c(\xi)} d\xi \right)^{-1} \quad (3.3)$$

and

$$\Phi(x) = \bar{c} \int_0^x \frac{1}{c(\xi)} d\xi, \quad x \in (0, 1). \quad (3.4)$$

Next, we define the transformation V by

$$Vf(x) = \psi(x)f(x), \quad (3.5)$$

where

$$\psi(x) = \exp \left[\frac{\bar{c}}{2} \int_0^x c'(\Phi^{-1}(\xi)) d\xi \right], \quad (3.6)$$

which yields

$$\begin{aligned}
A_s &= V^{-1} \bar{A} V f \\
&= V^{-1} \{ \bar{c}^2 [V f]_{xx} - \bar{c}(c' \circ \Phi^{-1}) [V f]_x \} \\
&= \psi^{-1} \{ \bar{c}^2 [\psi f'' + 2\psi' f' + \psi'' f] - \\
&\quad \bar{c}(c' \circ \Phi^{-1}) [\psi f' + \psi' f] \} \\
&= \bar{c}^2 f'' + \\
&\quad \left[2 \left(\frac{\psi'}{\psi} \right) \bar{c}^2 - \bar{c}(c' \circ \Phi^{-1}) \right] f' + \\
&\quad \left[\left(\frac{\psi''}{\psi} \right) \bar{c}^2 + \left(\frac{\psi'}{\psi} \right) \bar{c}(c' \circ \Phi^{-1}) \right] f \\
&= \bar{c}^2 f'' + \\
&\quad \left[\left(\left(\frac{\bar{c} c' \circ \Phi^{-1}}{2} \right)^2 + \frac{\bar{c}(c' \circ \Phi^{-1})'}{2} \right) \bar{c}^2 + \right. \\
&\quad \left. \frac{1}{2} (\bar{c} c' \circ \Phi^{-1})^2 \right] f
\end{aligned} \tag{3.7}$$

It is easy to see that these transformations have the property that they symmetrize the operator \mathcal{A} , and they also respect the boundary conditions; i.e., if $f \in \text{dom}(A) = H^2(0, 1) \cap H_0^1(0, 1)$, then $V(f \circ \Phi^{-1}) \in \text{dom}(A)$, and conversely.

3.2 Krylov Subspace Spectral Methods for IBVP

Once we have preconditioned the operator \mathcal{A} , to obtain a new self-adjoint operator $\tilde{\mathcal{A}}$, we can use Krylov subspace methods developed in [12] to compute an approximate solution. These methods are Galerkin methods that use an approximation for each coefficient of the solution in the chosen basis that is, in some sense, optimal.

3.2.1 Reduction to Quadratic Forms

Using a standard Galerkin approach, we begin with an orthonormal set of N trial functions

$$\phi_\omega(x) = \sqrt{2} \sin(\pi\omega x), \quad 0 < \omega \leq N, \tag{3.8}$$

that satisfy the boundary conditions. We seek an approximate solution

$$\tilde{u}(x, t) = \sum_{\omega=1}^N \tilde{u}_\omega(t) \phi_\omega(x), \tag{3.9}$$

that lies in the space spanned by the trial functions, where each coefficient \tilde{u}_ω , $\omega = 1, \dots, N$, is an approximation of the quantity

$$u_\omega(t) = \langle \phi_\omega, u(\cdot, t) \rangle. \quad (3.10)$$

Since the exact solution $u(x, t)$ is given by

$$u(x, t) = R_0(t)f(x) + R_1(t)g(x), \quad (3.11)$$

where $R_0(t)$ and $R_1(t)$ are defined in (2.7), (2.8), we can obtain \tilde{u}_ω by approximating each of the quadratic forms

$$c_\omega^+(t) = \langle \phi_\omega + \delta f, R_0(t)[\phi_\omega + \delta f] \rangle \quad (3.12)$$

$$c_\omega^-(t) = \langle \phi_\omega - \delta f, R_0(t)[\phi_\omega - \delta f] \rangle \quad (3.13)$$

$$s_\omega^+(t) = \langle \phi_\omega + \delta g, R_1(t)[\phi_\omega + \delta g] \rangle \quad (3.14)$$

$$s_\omega^-(t) = \langle \phi_\omega - \delta g, R_1(t)[\phi_\omega - \delta g] \rangle, \quad (3.15)$$

where δ is a nonzero constant, since

$$u_\omega(t) = \frac{c_\omega^+(t) - c_\omega^-(t)}{4\delta} + \frac{s_\omega^+(t) - s_\omega^-(t)}{4\delta}. \quad (3.16)$$

Similarly, we can obtain the coefficients \tilde{u}_ω of an approximation of $u_t(x, t)$ by approximating the quadratic forms

$$c_\omega^+(t)' = -\langle \phi_\omega + \delta f, AR_1(t)[\phi_\omega + \delta f] \rangle \quad (3.17)$$

$$c_\omega^-(t)' = -\langle \phi_\omega - \delta f, AR_1(t)[\phi_\omega - \delta f] \rangle \quad (3.18)$$

$$s_\omega^+(t)' = \langle \phi_\omega + \delta g, R_0(t)[\phi_\omega + \delta g] \rangle \quad (3.19)$$

$$s_\omega^-(t)' = \langle \phi_\omega - \delta g, R_0(t)[\phi_\omega - \delta g] \rangle. \quad (3.20)$$

As noted in [12], this approximation to $u_t(x, t)$ does not introduce *any* error due to differentiation of our approximation of $u(x, t)$ with respect to t —the latter approximation can be differentiated *analytically*.

It follows from the preceding discussion that we can compute an approximate solution $\tilde{u}(x, t)$ at a given time T using the following algorithm.

Algorithm 3.1 (Krylov Subspace Spectral Method for IBVP) *Given functions $c(x)$, $f(x)$, and $g(x)$ defined on the interval $(0, 1)$, a final time T , and an orthonormal set of functions $\{\phi_1, \dots, \phi_N\}$ that satisfy the boundary conditions, the following algorithm computes a function $\tilde{u}(x, t)$ of the form (3.9) that approximately solves the problem (1.1), (3.1) from $t = 0$ to $t = T$.*

$t = 0$

Choose a nonzero constant δ

while $t < T$ **do**

Select a time step Δt

$f(x) = \tilde{u}(x, t)$

$g(x) = \tilde{u}_t(x, t)$

for $\omega = 1$ **to** N **do**

Compute the quantities $c_\omega^+(\Delta t)$, $c_\omega^-(\Delta t)$, $s_\omega^+(\Delta t)$, $s_\omega^-(\Delta t)$,
 $c_\omega^+(\Delta t)'$, $c_\omega^-(\Delta t)'$, $s_\omega^+(\Delta t)'$, and $s_\omega^-(\Delta t)'$

$\tilde{u}_\omega(\Delta t) = \frac{1}{4\delta}(c_\omega^+(\Delta t) - c_\omega^-(\Delta t)) + \frac{1}{4\delta}(s_\omega^+(\Delta t) - s_\omega^-(\Delta t))$

$\tilde{v}_\omega(\Delta t) = \frac{1}{4\delta}(c_\omega^+(\Delta t)' - c_\omega^-(\Delta t)') + \frac{1}{4\delta}(s_\omega^+(\Delta t)' - s_\omega^-(\Delta t)')$

end

$\tilde{u}(x, t + \Delta t) = \sum_{\omega=1}^N \phi_\omega(x) \tilde{u}_\omega(\Delta t)$

$\tilde{u}_t(x, t + \Delta t) = \sum_{\omega=1}^N \phi_\omega(x) \tilde{v}_\omega(\Delta t)$

$t = t + \Delta t$

end

3.2.2 Computation of the Quadratic Forms

We now discuss the approximation of quantities of the form

$$I[f] = \langle v_N, f(A)v_N \rangle \quad (3.21)$$

where A is the $L_2(0, 1)$ -realization of a self-adjoint differential operator \mathcal{A} defined on $\text{dom}(A) = H^2(0, 1) \cap H_0^1(0, 1)$, f is a given analytic function and $v_N(x)$ is a function of the form

$$v_N(x) = \sum_{\omega=1}^N u_\omega \phi_\omega(x). \quad (3.22)$$

Given this representation of v_N , we can approximate this quantity by

$$I_N[f] = \mathbf{v}_N^T f(A_N) \mathbf{v}_N \quad (3.23)$$

where $\mathbf{v}_N = [v_N(x_1) \ \cdots \ v_N(x_N)]^T$, and A_N is an $N \times N$ symmetric matrix that approximates the operator A on the space spanned by $\{\phi_1, \dots, \phi_N\}$. For example, we may choose

$$[A_N]_{ij} = \sum_{k,\ell=1}^N \phi_k(x_i) \langle \phi_k, A\phi_\ell \rangle \phi_\ell(x_j), \quad (3.24)$$

or use a finite-difference approximation that takes the boundary conditions into account. In particular, if we use a three-point stencil, then A_N is a tridiagonal matrix.

We can compute this quadratic form using techniques described in [4]. Let A_N have eigenvalues

$$a = \lambda_1 \geq \dots \geq \lambda_N = b, \quad (3.25)$$

with corresponding eigenvectors $\mathbf{q}_1, \dots, \mathbf{q}_N$. Then

$$I_N[f] = \mathbf{v}_N^T f(A_N) \mathbf{v}_N \quad (3.26)$$

$$= \sum_{j=1}^N f(\lambda_j) |\mathbf{q}_j^T \mathbf{v}_N|^2 \quad (3.27)$$

$$= \int_a^b f(\lambda) d\alpha(\lambda) \quad (3.28)$$

where $\alpha(\lambda)$ is the piecewise constant measure

$$\alpha(\lambda) = \begin{cases} 0 & \lambda < a \\ \sum_{j=i}^n |\mathbf{q}_j^T \mathbf{v}_N|^2 & \lambda_i \leq \lambda < \lambda_{i+1} \\ \sum_{j=1}^n |\mathbf{q}_j^T \mathbf{v}_N|^2 & b \leq \lambda \end{cases} . \quad (3.29)$$

We can approximate the value of this Riemann-Stieltjes integral using Gaussian quadrature. Applying the symmetric Lanczos algorithm to A_N with initial vector \mathbf{v}_N , we can construct a sequence of polynomials p_1, \dots, p_K that are orthogonal with respect to the measure $\alpha(\lambda)$. These polynomials satisfy a three-term recurrence relation

$$\beta_{j+1} p_{j+1}(\lambda) = (\lambda - \alpha_{j+1}) p_j(\lambda) - \beta_j p_{j-1}(\lambda), \quad (3.30)$$

$$p_{-1}(\lambda) \equiv 0, \quad p_0(\lambda) = \frac{1}{\|\mathbf{v}_N\|_2}, \quad (3.31)$$

which can be written in matrix-vector notation as

$$\lambda \mathbf{p}_K(\lambda) = J_K \mathbf{p}_K(\lambda) + \beta_K p_K(\lambda) \mathbf{e}_K \quad (3.32)$$

where

$$\mathbf{p}_K(\lambda) = \begin{bmatrix} p_0(\lambda) \\ \vdots \\ p_{K-1}(\lambda) \end{bmatrix}, \quad J_K = \begin{bmatrix} \alpha_1 & \beta_1 & & & & \\ \beta_1 & \alpha_2 & \beta_1 & & & \\ & \ddots & \ddots & \ddots & & \\ & & \ddots & \ddots & \beta_{K-1} & \\ & & & \beta_{K-1} & \alpha_K & \end{bmatrix}. \quad (3.33)$$

It follows that the eigenvalues of J_K are the zeros of $p_K(\lambda)$, which are the nodes for Gaussian quadrature. It can be shown (see [8]) that the corresponding weights are equal to the squares of the first components of the normalized eigenvectors of J_K .

3.2.3 Accuracy of the Approximate Solution

We now state and prove a result concerning the accuracy of each component of the approximate solution. We first use the following result from [12].

Lemma 3.2 *Let A be an $N \times N$ symmetric positive definite matrix. Let \mathbf{u} and \mathbf{v} be fixed vectors, and define $\mathbf{u}_\delta = \mathbf{u} + \delta\mathbf{v}$. For j a positive integer, let $\tilde{g}_j(\delta)$ be defined by*

$$\tilde{g}_j(\delta) = \frac{1}{2} \mathbf{e}_1^T T_\delta^j \mathbf{e}_1 \|\mathbf{u}_\delta\|_2^2, \quad (3.34)$$

where T_δ is the $K \times K$ Jacobi matrix produced by the K iterations of the symmetric Lanczos algorithm applied to A with starting vector \mathbf{u}_δ . Then, for some η satisfying $0 < \eta < \delta$,

$$\begin{aligned} \frac{\tilde{g}_j(\delta) - \tilde{g}_j(-\delta)}{2\delta} &= \mathbf{u}^T A^j \mathbf{v} + \\ &\sum_{k=K}^{j-K} \mathbf{e}_1^T \left[T^k X^T - X^T A^k \right]' \mathbf{r}_K^T T^{j-k-1} \mathbf{e}_1 \mathbf{u}^T \mathbf{u} + \\ &\frac{\delta^2}{6} \left[\sum_{k=K}^{j-K} \mathbf{e}_1^T \left[T_\delta^k X_\delta^T - X_\delta^T A^k \right]' \mathbf{r}_\delta^T \mathbf{e}_K^T T_\delta^{j-k-1} \mathbf{e}_1 \mathbf{u}_\delta^T \mathbf{u}_\delta \right]'' \Bigg|_{\delta=\eta} \end{aligned} \quad (3.35)$$

Proof See [12]. \square

Corollary 3.3 *Under the assumptions of the lemma,*

$$\frac{\tilde{g}_j(\delta) - \tilde{g}_j(-\delta)}{2\delta} = \mathbf{u}^T A^j \mathbf{v}, \quad (3.36)$$

for $0 \leq j < 2K$.

We can now describe the local truncation error of each component of the computed solution.

Theorem 3.4 *Assume that $c(x)^2$, $f(x)$, and $g(x)$ belong to $\text{span}\{\phi_1, \dots, \phi_N\}$, and let $u(x, \Delta t)$ be the exact solution of (1.1), (3.1) at $(x, \Delta t)$, and let $\tilde{u}(x, \Delta t)$ be the approximate solution computed by Algorithm 3.1. Then*

$$|\langle \phi_\omega, u(\cdot, \Delta t) - \tilde{u}(\cdot, \Delta t) \rangle| = O(\Delta t^{4K}) \quad (3.37)$$

where K is the number of quadrature nodes used in Algorithm 3.1.

Proof Let $\tilde{g}(\delta)$ be the function from Lemma 3.2 with $A = A_{N_K}$, where $N_K = 2^K N$, $\mathbf{u} = \phi_\omega$ and $\mathbf{v} = \mathbf{f}$, where $\mathbf{f} = [f(x_1) \ \cdots \ f(x_{N_K})]^T$. Furthermore, denote the entries of T_δ by

$$T_\delta = \begin{bmatrix} \alpha_1(\delta) & \beta_1(\delta) & & & & \\ \beta_1(\delta) & \alpha_2(\delta) & \beta_2(\delta) & & & \\ & \ddots & \ddots & \ddots & & \\ & & & \beta_{K-2}(\delta) & \alpha_{K-1}(\delta) & \beta_{K-1}(\delta) \\ & & & & \beta_{K-1}(\delta) & \alpha_K(\delta) \end{bmatrix}. \quad (3.38)$$

Finally, let $\beta_0(\delta) = \|\mathbf{u}_\delta\|_2$ and $\beta_K(\delta) = \|\mathbf{r}_\delta\|_2$, and let

$$c_\omega = \frac{1}{4\delta} [c_\omega^+(\Delta t) - c_\omega^-(\Delta t)] = \langle \phi_\omega, \tilde{R}_0(\Delta t) f \rangle. \quad (3.39)$$

Then, by Lemma 3.2 and Corollary 3.3,

$$\begin{aligned}
\langle \phi_\omega, R_0(\Delta t)f \rangle - c_\omega &= \sum_{j=0}^{\infty} (-1)^j \frac{\Delta t^{2j}}{(2j)!} \left\{ \langle \phi_\omega, A^j f \rangle - \frac{\tilde{g}_j(\delta) - \tilde{g}_j(-\delta)}{2\delta} \right\} \\
&= \sum_{j=0}^{\infty} (-1)^j \frac{\Delta t^{2j}}{(2j)!} \left\{ \langle \phi_\omega, A^j f \rangle - \mathbf{c}_\omega^T A_{N_K}^j \mathbf{f} + \right. \\
&\quad \left. \sum_{k=K}^{j-K} \mathbf{e}_1^T \frac{d}{d\delta} \left[T_\delta^k X_\delta^T - X_\delta^T A_{N_K}^k \right] \Big|_{\delta=0} \mathbf{r}_K^T T^{j-k-1} \mathbf{e}_1 \right\} + \\
&\quad O(\delta \Delta t^{4K}) \\
&= \frac{\Delta t^{4K}}{(4K)!} \mathbf{e}_1^T \frac{d}{d\delta} \left[T_\delta^K X_\delta^T - X_\delta^T A_{N_K}^K \right] \Big|_{\delta=0} \mathbf{r}_K^T T^{K-1} \mathbf{e}_1 + \\
&\quad O(\delta \Delta t^{4K}) \\
&= \frac{\Delta t^{4K}}{(4K)!} \mathbf{e}_1^T \frac{d}{d\delta} \left[\sum_{j=0}^{K-1} T_\delta^j \mathbf{e}_K \mathbf{r}_\delta^T A_{N_K}^{K-j-1} \right] \Big|_{\delta=0} \mathbf{r}_K^T T^{K-1} \mathbf{e}_1 + \\
&\quad O(\delta \Delta t^{4K}) \\
&= \frac{\Delta t^{4K}}{(4K)!} \mathbf{e}_1^T \frac{d}{d\delta} \left[T_\delta^{K-1} \mathbf{e}_K \mathbf{r}_\delta^T \right] \Big|_{\delta=0} \mathbf{r}_K^T T^{K-1} \mathbf{e}_1 + O(\delta \Delta t^{4K}) \\
&= \frac{1}{2} \frac{\Delta t^{4K}}{(4K)!} \frac{d}{d\delta} \left[\|\mathbf{r}_\delta\| \mathbf{e}_1^T T_\delta^{K-1} \mathbf{e}_K \right]^2 \Big|_{\delta=0} + O(\delta \Delta t^{4K}) \\
&= \frac{1}{2} \frac{\Delta t^{4K}}{(4K)!} \frac{d}{d\delta} (\beta_0(\delta) \cdots \beta_K(\delta))^2 \Big|_{\delta=0} + O(\delta \Delta t^{4K}) \\
&= O(\Delta t^{4K}). \tag{3.40}
\end{aligned}$$

A similar result holds for $s_\omega = \langle \phi_\omega, \tilde{R}_1(\Delta t)g \rangle$. \square

Note that the proof assumes that Algorithm 3.1 uses a discretization of A on an N_K -point grid, where $N_K = 2^K N$. This grid refinement is used to avoid loss of information that would be incurred on an N -point grid when multiplying gridfunctions. In practice this refinement is seen to be unnecessary when the coefficients are reasonably smooth. When it is needed to ensure sufficient accuracy, its effect on the efficiency of Algorithm 3.1 is minimized by the fact that K is typically chosen to be small (say, $K = 2$ or $K = 3$). Implementation details discussed in [13] also mitigate this concern.

3.2.4 Non-Orthogonal Basis Functions

Ideally, we would like our trial functions to be approximate eigenfunctions of the symmetrized operator $\tilde{\mathcal{A}}$ obtained previously. Although the eigenfunctions of this operator are orthogonal with respect to the inner product $\langle \cdot, \cdot \rangle$, we cannot assume that any basis of approximate eigenfunctions is necessarily orthogonal as well.

Suppose that we refine our initial (orthogonal) basis of approximate eigenfunctions of the form (3.8) to obtain a new basis $\{\tilde{\phi}_\omega(x)\}_{\omega=1}^{N-1}$ so that each function $\tilde{\phi}_\omega(x)$ is a sparse combination of functions of the form (3.8); i.e.,

$$\tilde{\Phi} = \Phi C \quad (3.41)$$

where the matrices $\tilde{\Phi}$ and Φ are defined by

$$\Phi_{ij} = \phi_j(x_i), \quad \tilde{\Phi}_{ij} = \tilde{\phi}_j(x_i), \quad x_i = i\Delta x, \quad 0 < i < N, \quad (3.42)$$

and the matrix C is sparse. Then, if we define the vector $\mathbf{u}(t)$ to be the values of our approximate solution $\tilde{u}(x, t)$ at time t and the gridpoints x_i , $i = 1, \dots, N-1$, then we can efficiently obtain $\mathbf{u}(t + \Delta t)$ by computing

$$\mathbf{u}(t + \Delta t) = \Phi C (C^T C)^{-1} \tilde{\mathbf{u}}(t + \Delta t) \quad (3.43)$$

where the vector $\tilde{\mathbf{u}}(t + \Delta t)$ is defined by

$$[\tilde{\mathbf{u}}(t + \Delta t)]_\omega = \langle \tilde{\phi}_\omega, \tilde{R}_0(t)\tilde{u}(\cdot, t) + \tilde{R}_1(t)\tilde{u}_t(\cdot, t) \rangle, \quad 0 < \omega < N. \quad (3.44)$$

Generalizing, if we obtain the matrix $\tilde{\Phi}$ representing the values of approximate eigenfunctions by a sequence of transformations C_1, \dots, C_k where each C_j , $j = 1, \dots, k$, has $O(1)$ bandwidth, and the integer k is small, then we can still compute the solution in $O(N)$ time per time step.

3.3 Numerical Experiments

To test our algorithm we solve the problem (1.1), (3.1) from $t = 0$ to $t = 1$.

3.3.1 Construction of Test Cases

In many of the following experiments, it is necessary to construct functions of a given smoothness. To that end, we rely on the following result (see [9]):

Theorem 3.5 *Let $f(x)$ be a 2π -periodic function and assume that its p th derivative is a piecewise C^1 function. Then,*

$$|\hat{f}(\omega)| \leq \text{constant}/(|\omega|^{p+1} + 1). \quad (3.45)$$

Based on this result, the construction of a C^{p+1} function $f(x)$ proceeds as follows:

1. For each $\omega = 1, \dots, N/2 - 1$, choose the discrete Fourier coefficient $\hat{f}(\omega)$ by setting $\hat{f}(\omega) = (u + iv)/|\omega^{p+1} + 1|$, where u and v are random numbers uniformly distributed on the interval $(0, 1)$.
2. For each $\omega = 1, \dots, N/2 - 1$, set $\hat{f}(-\omega) = \overline{\hat{f}(\omega)}$.
3. Set $\hat{f}(0)$ equal to any real number.
4. Set $f(x) = \sum_{|\omega| < N/2} \hat{f}(\omega) e^{2\pi i \omega x}$.

In the following test cases, coefficients and initial data are constructed so that their third derivatives are piecewise C^1 , unless otherwise noted.

We will now introduce some functions that will be used in the experiments described in this section. As these functions and operators are randomly generated, we will denote by R_1, R_2, \dots the sequence of random numbers obtained using MATLAB's random number generator `rand` after setting the generator to its initial state. These numbers are uniformly distributed on the interval $(0, 1)$.

We will make frequent use of a two-parameter family of functions defined on the interval $[0, 1]$. First, we define

$$f_{j,k}^0(x) = \operatorname{Re} \left\{ \sum_{|\omega| < N/2, \omega \neq 0} \hat{f}_j(\omega) (1 + |\omega|)^{k+1} e^{i\omega x} \right\}, \quad j, k = 0, 1, \dots, \quad (3.46)$$

where

$$\hat{f}_j(\omega) = R_{jN+2(\omega+N/2)-1} + iR_{jN+2(\omega+N/2)}. \quad (3.47)$$

The parameter j indicates how many functions have been generated in this fashion since setting MATLAB's random number generator to its initial state, and the parameter k indicates how smooth the function is.

In many cases, it is necessary to ensure that a function is positive or negative, so we define the translation operators E^+ and E^- by

$$E^+ f(x) = f(x) - \min_{x \in [0,1]} f(x) + 1, \quad (3.48)$$

$$E^- f(x) = f(x) - \max_{x \in [0,1]} f(x) - 1. \quad (3.49)$$

It is also necessary to ensure that a periodic function vanishes on the boundary, so we define the translation operator E_0 by

$$E^0 f(x) = f(x) - f(0). \quad (3.50)$$

3.3.2 Discretization and Error Estimation

The problem is solved using the following methods:

- A finite difference scheme presented by Kreiss, et. al. (see [11]).
- The Krylov subspace spectral method with $K = 2$ Gaussian quadrature nodes and the basis (3.8).
- The Krylov subspace spectral method with $K = 2$ Gaussian quadrature nodes and a basis obtained by applying two iterations of inverse iteration to each function in the basis (3.8).

In all cases, the operator $\mathcal{A} = c(x)^2 \partial_{xx}$ is preconditioned using the transformations described in Section 2 to obtain a self-adjoint operator $\tilde{\mathcal{A}}$. Then, the $L_2(0, 1)$ -realization of $\tilde{\mathcal{A}}$ defined on $H^2(0, 1) \cap H_0^1(0, 1)$ is discretized using a matrix of the form (3.24) that operates on the space of gridfunctions defined on a grid consisting of N equally spaced points $x_j = j\Delta x$, where $\Delta x = 1/(N + 1)$, for various values of N .

The approximate solution is then computed using time steps $\Delta t_k = 2^{-k}$, $k = 0, \dots, 6$, so that we can analyze the temporal convergence behavior. Let $u^{(k)}(x, t)$, $k = 0, \dots, 6$, be the approximate solution computed using time step Δt_k . For $k = 0, \dots, 6$, the relative error E_k in $u^{(k)}(x, t)$ at $t = 1$ is estimated as follows: We use the same method to solve the *backward problem* for (1.1) with end conditions

$$u(x, 1) = u^{(k)}(x, t), \quad u_t(x, 1) = -u_t^{(k)}(x, t), \quad x \in (0, 1). \quad (3.51)$$

Let $v^{(k)}(x, t)$ be the approximation solution of the inverse problem, for $k = 0, \dots, 6$. Then we approximating the relative difference between $v^{(k)}(x, 0)$ and $u^{(k-1)}(x, 0) = f(x)$ in the L_2 -norm; i.e.,

$$E_k \approx \frac{\|\mathbf{u}^{(k)}(\cdot, 0) - \mathbf{v}^{(k)}(\cdot, 0)\|_2}{\|\mathbf{u}^{(k)}(\cdot, 0)\|_2}, \quad (3.52)$$

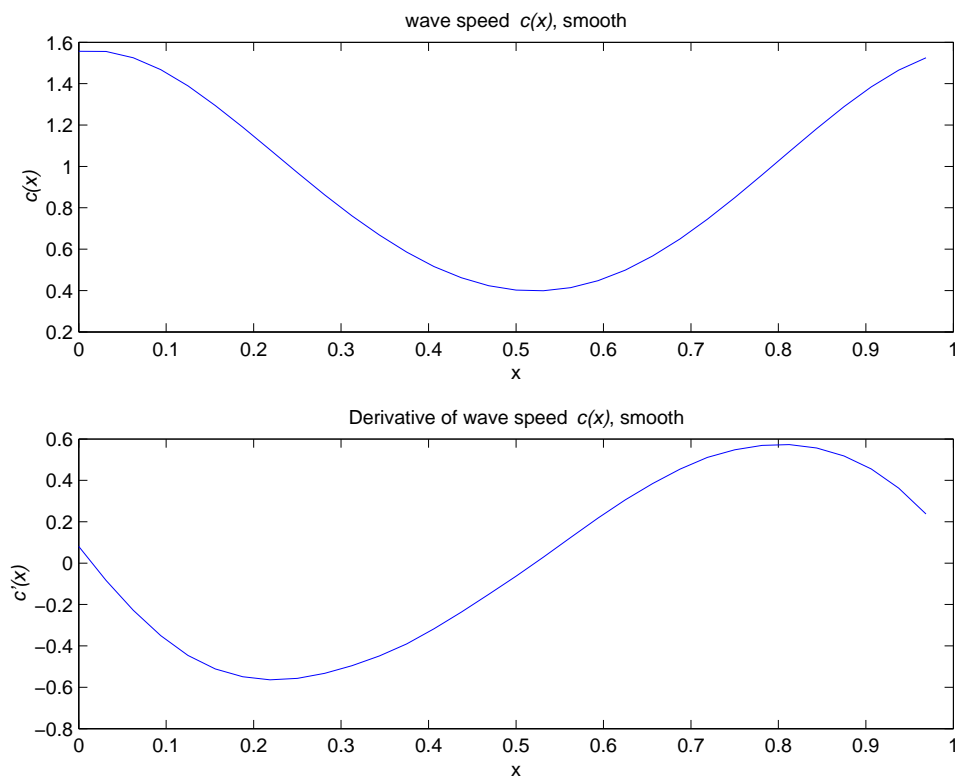
where

$$[\mathbf{u}^{(k)}]_j = u^{(k)}(x_j, 0), \quad [\mathbf{v}^{(k)}]_j = v^{(k)}(x_j, 0), \quad x_j = j\Delta x. \quad (3.53)$$

3.3.3 Results

We first solve the problem (1.1), (3.1) with smooth data

$$c(x) = f_{0,3}(x), \quad f(x) = f_{1,3}(x), \quad g(x) = f_{2,3}(x). \quad (3.54)$$

Figure 1: Smooth wave speed $c(x) = f_{0,3}(x)$

The functions $c(x)$, $f(x)$, and $g(x)$ are plotted in Figures 1, 2, and 3, respectively.

The temporal convergence is illustrated in Figure 4, where $N = 31$ grid-points are used in all cases. The finite difference method of Kreiss, et. al. converges quadratically, whereas approximately 6th-order convergence is attained using the Krylov subspace spectral method. Note that the use of inverse iteration does not improve the convergence rate, but it does yield a more accurate approximation for larger time steps.

In Figure 5, all three methods are used to solve (1.1), (3.1) with time steps $\Delta t_k = 2^{-k}$ and mesh sizes $\Delta x_k = 2^{-(k+5)}$, for $k = 0, \dots, 3$. The finite-difference method converges quadratically, while the Krylov subspace spectral method without inverse iteration exhibits quintic convergence. Using inverse iteration, the convergence is only superquadratic, but this is due to the fact that the accuracy is so high at $\Delta t_0 = 1$ that the machine precision prevents attaining a faster convergence rate for smaller time steps.

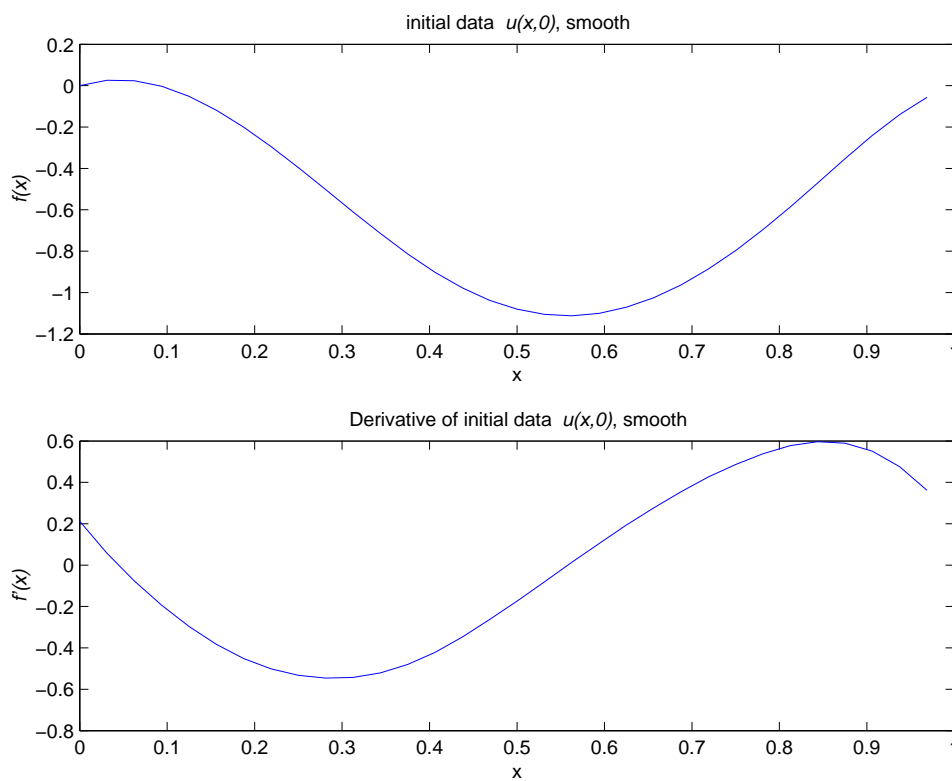


Figure 2: Smooth initial data $u(x,0) = f(x) = f_{1,3}(x)$

Both experiments are repeated with data that is not as smooth. Specifically, we use

$$c(x) = f_{0,1}(x), \quad f(x) = f_{1,1}(x), \quad g(x) = f_{2,1}(x). \quad (3.55)$$

The functions $c(x)$, $f(x)$, and $g(x)$ are plotted in Figures 6, 7, and 8, respectively. The results corresponding to Figures 4 and 5 are illustrated in Figures 9 and 10, respectively. As expected, the accuracy and the convergence rate are impaired to some extent. This can be alleviated by refining the spatial grid during the Lanczos iteration, as described in [12], in order to obtain more accurate inner products of functions; we do not do this here.

3.4 Gaussian Quadrature in the Spectral Domain

Consider the computation of the quadratic form $\langle \phi_\omega, f(\tilde{A})\phi_\omega \rangle$ where $\phi_\omega(x)$ is defined in (3.8) and \tilde{A} is defined in (3.7). Figures 11 and 12 illustrate

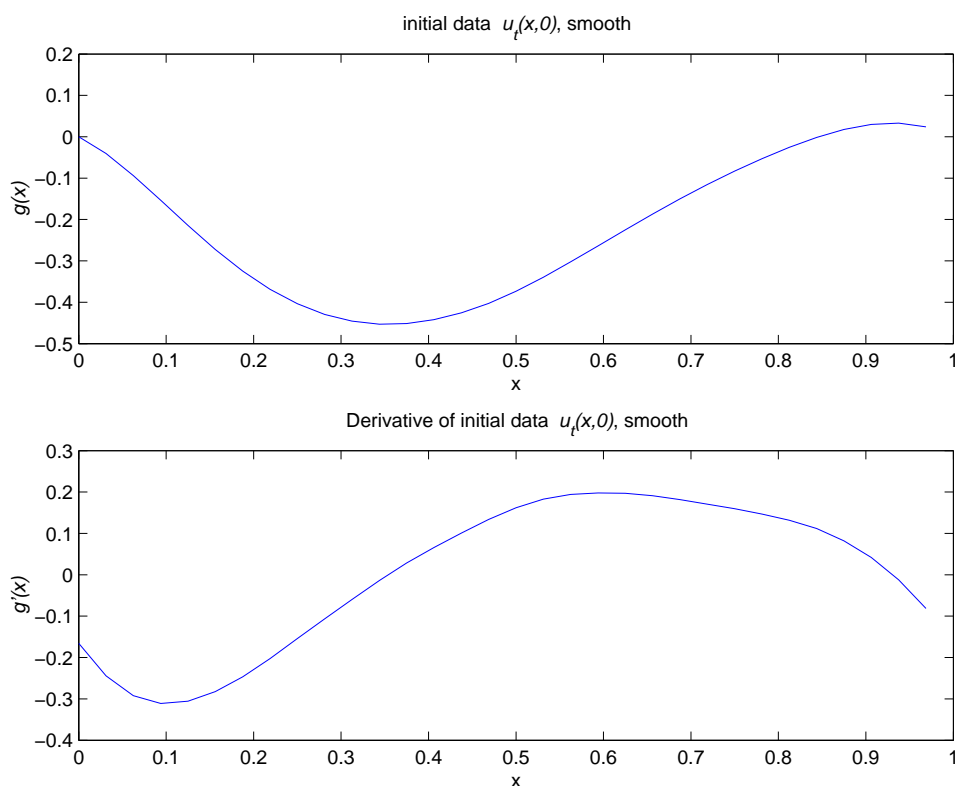


Figure 3: Smooth initial data $u_t(x, 0) = g(x) = f_{2,3}(x)$

the relationship between the eigenvalues of \tilde{A} and the Gaussian quadrature nodes obtained by the symmetric Lanczos algorithm that is employed by Krylov subspace spectral methods. In Figure 11, the speed $c(x)$ is defined to be $c_{3,1}(x)$, which is shown in Figure 1. Since the speed is smooth, $\phi_\omega(x)$ is an approximate eigenfunction of \tilde{A} , and it follows that the nodes are clustered around the corresponding approximate eigenvalue. In Figure 12, the speed is $c(x) = 1 + \frac{1}{2} \cos(32\pi x)$. Because of this oscillatory perturbation, the eigenvalues do not define a smooth curve, as seen in the top plot. Note that the sharp oscillations in the curve traced by the eigenvalues correspond to sharp changes in the placement of the two quadrature nodes.

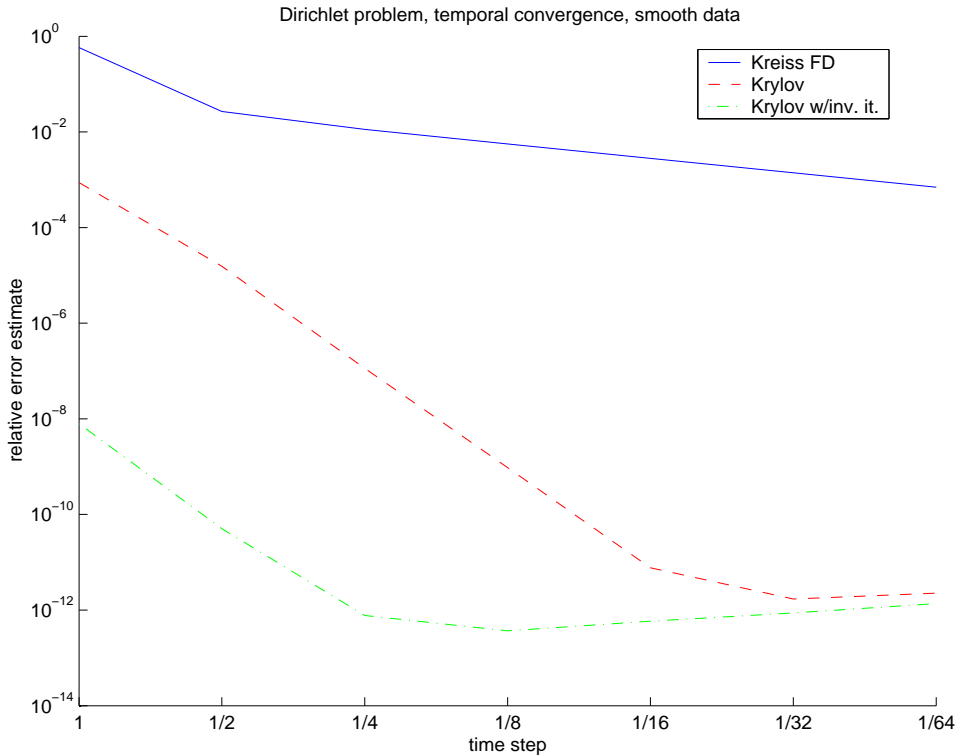


Figure 4: Estimates of relative error in approximate solutions of the problem (1.1), (3.1) with data (3.54) computed using finite differencing and Krylov subspace spectral methods, with time steps $\Delta t_k = 2^{-k}$, $k = 0, \dots, 6$.

4 Conclusions

We have considered wave propagation in one dimension in the case of heterogeneous and complicated coefficients. Our point of view has been to consider the analytical structure of the solution operator in order to derive asymptotic properties for the spectrum. In particular, we considered non-selfadjoint problems with small fluctuations in the coefficients and problems where the fluctuations are large and rapid, respectively. We then derived techniques for efficient and accurate numerical wave propagation that are based on using low-dimensional Krylov subspace approximations of the solution operator to obtain components of the solution in a basis of trial functions in a Galerkin-type scheme. We demonstrated that this approach gives a high-order approximation which converges faster than competing methods

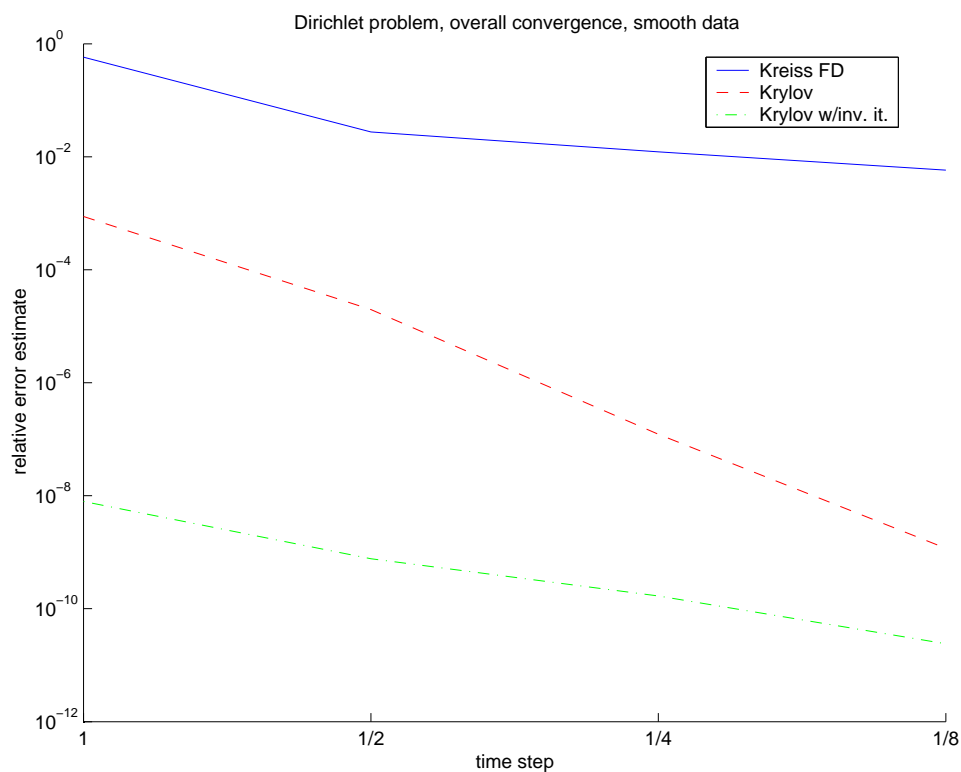


Figure 5: Estimates of relative error in approximate solutions of the problem (1.1), (3.1) with data (3.54) computed using finite differencing and Krylov subspace spectral methods, with time steps $\Delta t_k = 2^{-k}$ and mesh sizes $\Delta x_k = 2^{-(k+5)}$, for $k = 0, \dots, 3$.

in the problems that we have considered.

Developing theory and numerical procedures for wave propagation in rough and multiscale media is important in a number of applications, such as analysis and design of algorithms for solving inverse problems related to propagation in the ocean, the atmosphere or in the heterogeneous earth, for instance. Such applications require us, however, to consider propagation in several spatial dimensions, and our main aim is to generalize and integrate further our approach to deal with multiple spatial dimensions.

References

- [1] A. BENSOUSSAN, J. L. LIONS AND G. PAPANICOLAOU, “Asymptotic

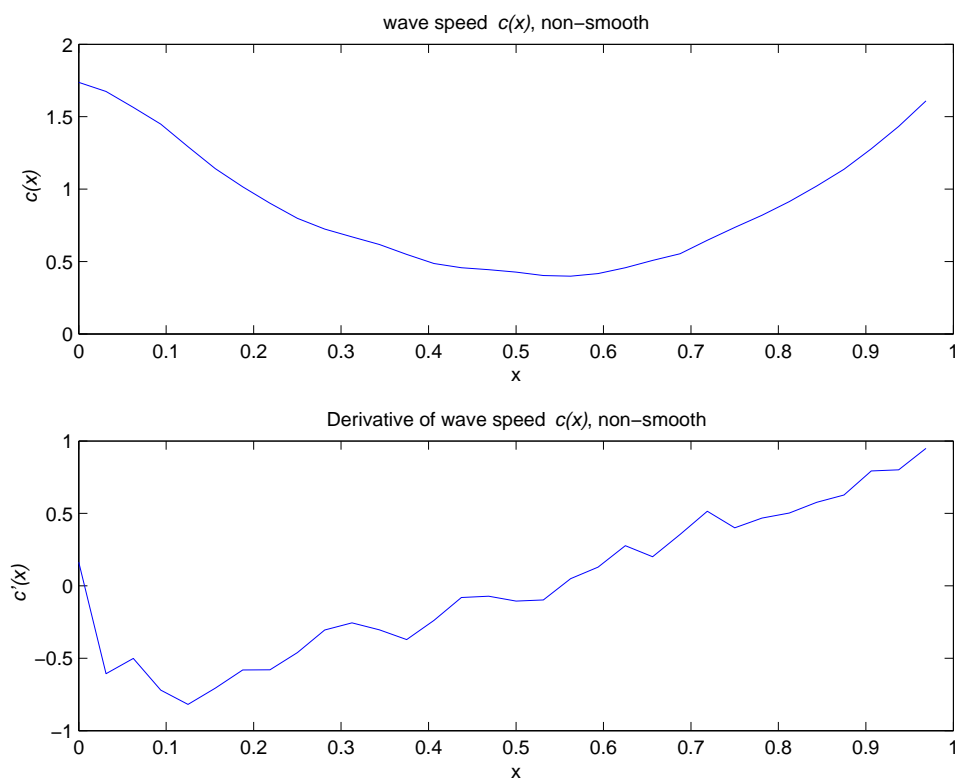


Figure 6: Non-smooth wave speed $c(x) = f_{0,1}(x)$

Analysis of Periodic Structures”, *North Holland*, (1978).

- [2] P. G. CASAZZA, “The art of frame theory”, *Taiwanese J. Math.* **4**(2) (2000), 129–201.
- [3] N. DUNFORD AND J. T. SCHWARZ, “Linear Operators, Part III”, *Wiley*, New York (1971).
- [4] G. DAHLQUIST, S. C. EISENSTAT AND G. H. GOLUB, “Bounds for the error of linear systems of equations using the theory of moments”, *J. Math. Anal. Appl.* **37** (1972), 151-166.
- [5] G. H. GOLUB, “Bounds for matrix moments”, *Rocky Mnt. J. of Math.* **4** (1974), 207-211.
- [6] G. H. GOLUB, “Some modified matrix eigenvalue problems”, *SIAM Review* **15** (1973) 318-334.

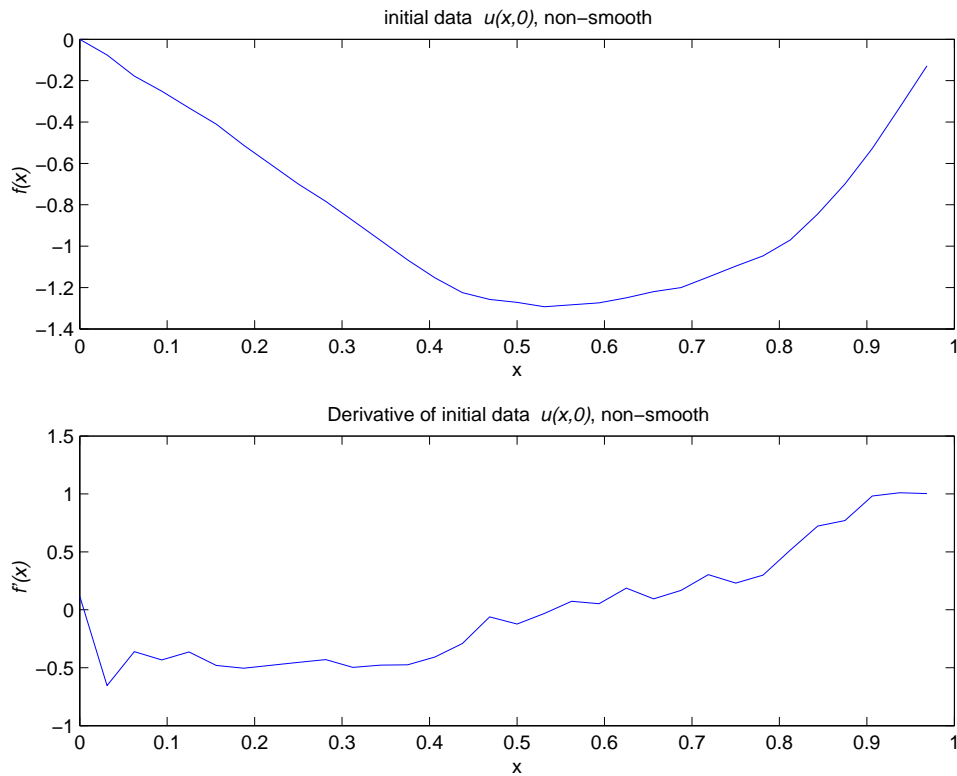


Figure 7: Non-smooth initial data $u(x,0) = f(x) = f_{1,1}(x)$

- [7] G. H. GOLUB AND C. MEURANT, “Matrices, Moments and Quadrature”, Stanford University Technical Report SCCM-93-07, (1993)
- [8] G. H. GOLUB AND J. WELSCH, “Calculation of Gauss Quadrature Rules”, *Math. Comp.* **23** (1969), 221-230.
- [9] B. GUSTAFSSON, H.-O. KREISS AND J. OLIGER, *Time-Dependent Problems and Difference Methods New York: Wiley*, (1995)
- [10] J. B. KELLER, D. MCLAUGHLIN AND G. PAPANICOLAOU, “Surveys in Applied Mathematics”, Plenum Press, (1995).
- [11] H.-O. KREISS, N. A. PETERSSON AND J. YSTRÖM, “Difference Approximations for the Second Order Wave Equation”, *SIAM J. Numer. Anal.* **40** (2002), 1940-1967.

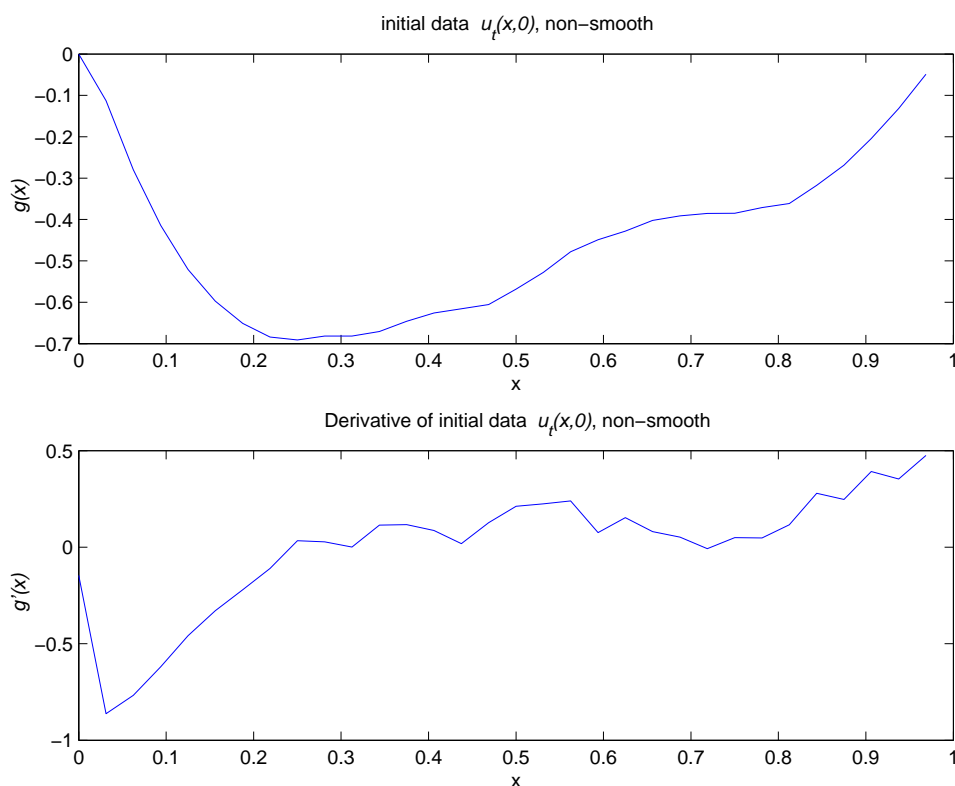


Figure 8: Non-smooth initial data $u_t(x, 0) = g(x) = f_{2,1}(x)$

- [12] J. V. LAMBERS, *Krylov Subspace Methods for Variable-Coefficient Initial-Boundary Value Problems*, Ph.D. Thesis, Stanford University SCCM Program, (2003).
- [13] J. V. LAMBERS, “Practical Implementation of Krylov Subspace Spectral Methods”, in preparation.
- [14] G. MILTON, “The Theory of Composites”, (2002).
- [15] K. SØLNA AND G. MILTON, “Can mixing materials make electromagnetic signals travel faster?”, *SIAM Journal on Applied Mathematics*, V 62, 6, (2002), 2064-2091.
- [16] G. SZEGO, “Orthogonal Polynomials”, 3rd. Ed. (1974) *Amer. Math. Soc.*

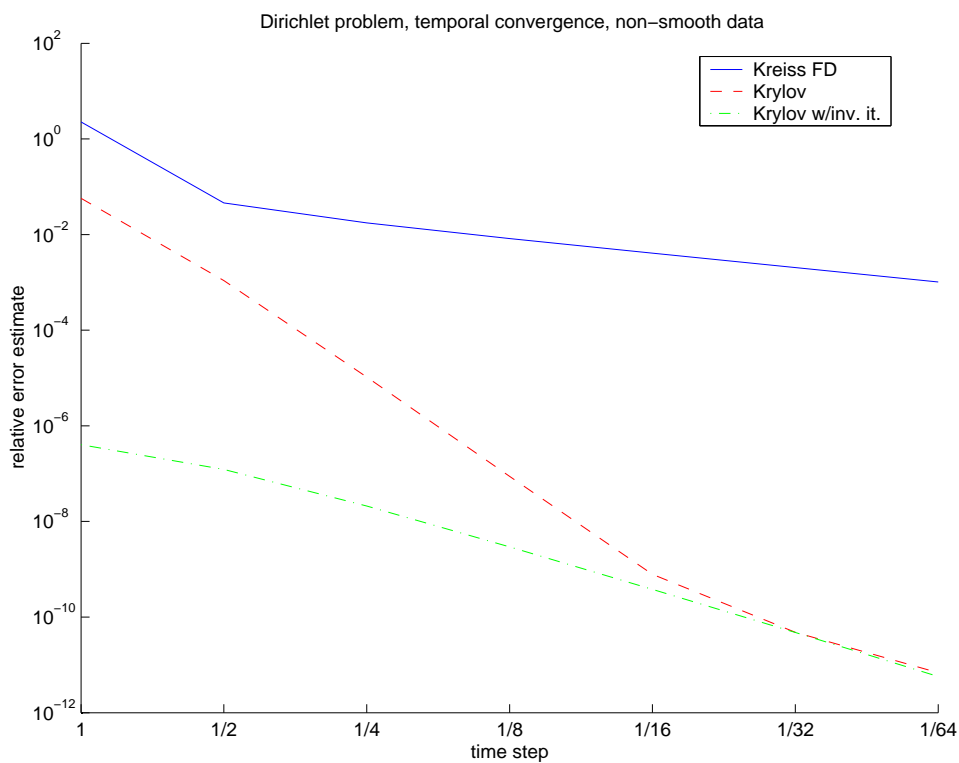


Figure 9: Estimates of relative error in approximate solutions of the problem (1.1), (3.1) with data (3.55) computed using finite differencing and Krylov subspace spectral methods, with time steps $\Delta t_k = 2^{-k}$, $k = 0, \dots, 6$.

- [17] YU. SAFAROV AND D. VASSILIEV, “The Asymptotic Distributions of Eigenvalues of Partial Differential Operators”, *Translation of Mathematical Monographs*, AMS (1997)

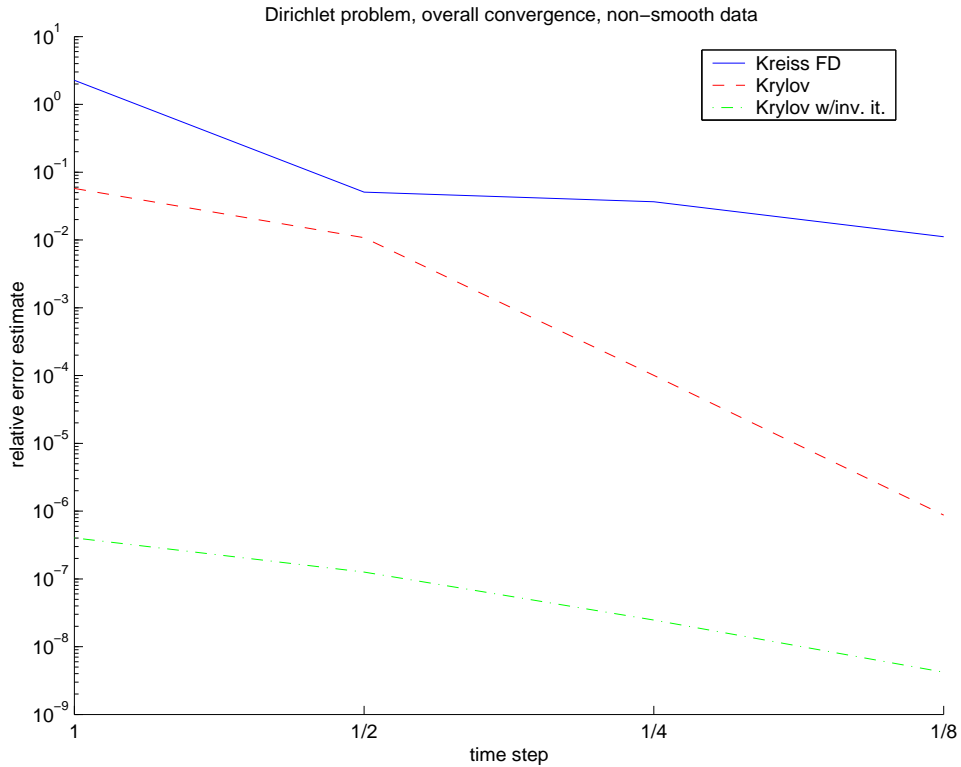


Figure 10: Estimates of relative error in approximate solutions of the problem (1.1), (3.1) with data (3.54) computed using finite differencing and Krylov subspace spectral methods, with time steps $\Delta t_k = 2^{-k}$ and mesh sizes $\Delta x_k = 2^{-(k+5)}$, for $k = 0, \dots, 3$.

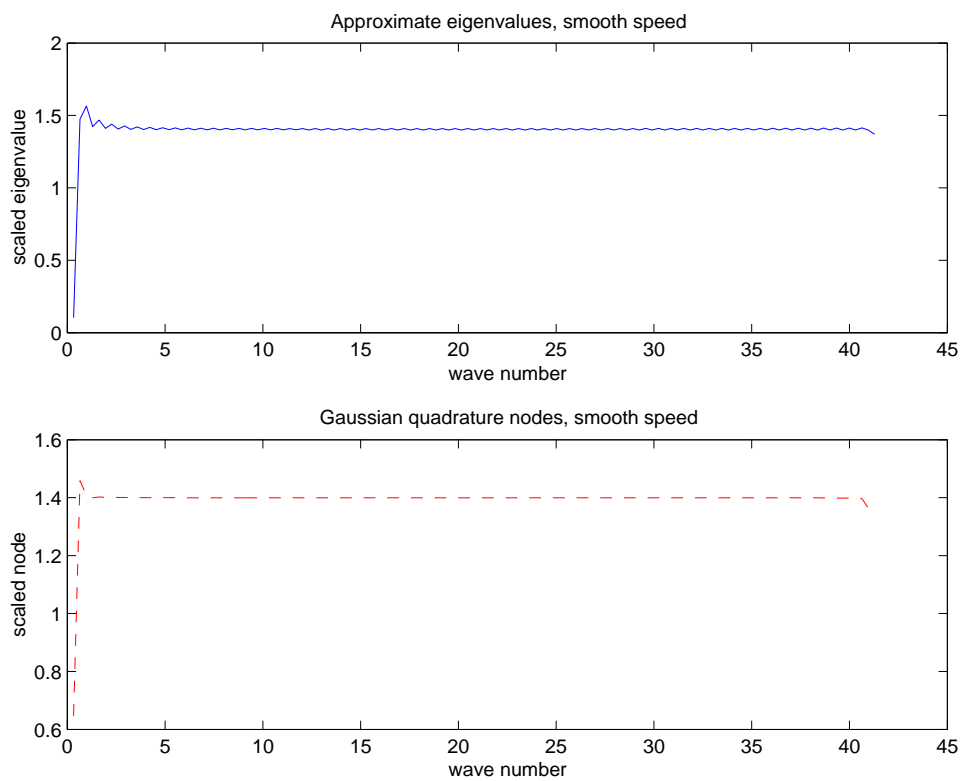


Figure 11: Approximate eigenvalues of the operator $\mathcal{A} = c_{3,1}(x)\partial_{xx}$, and Gaussian quadratures nodes of a 2-point rule used to approximate $\langle \phi_\omega, f(\tilde{\mathcal{A}})\phi_\omega \rangle$ where $\tilde{\mathcal{A}}$ is defined in (3.7), plotted against the wave number ω . For each eigenvalue, the wave number is determined by the dominant frequency of the corresponding approximate eigenfunction.

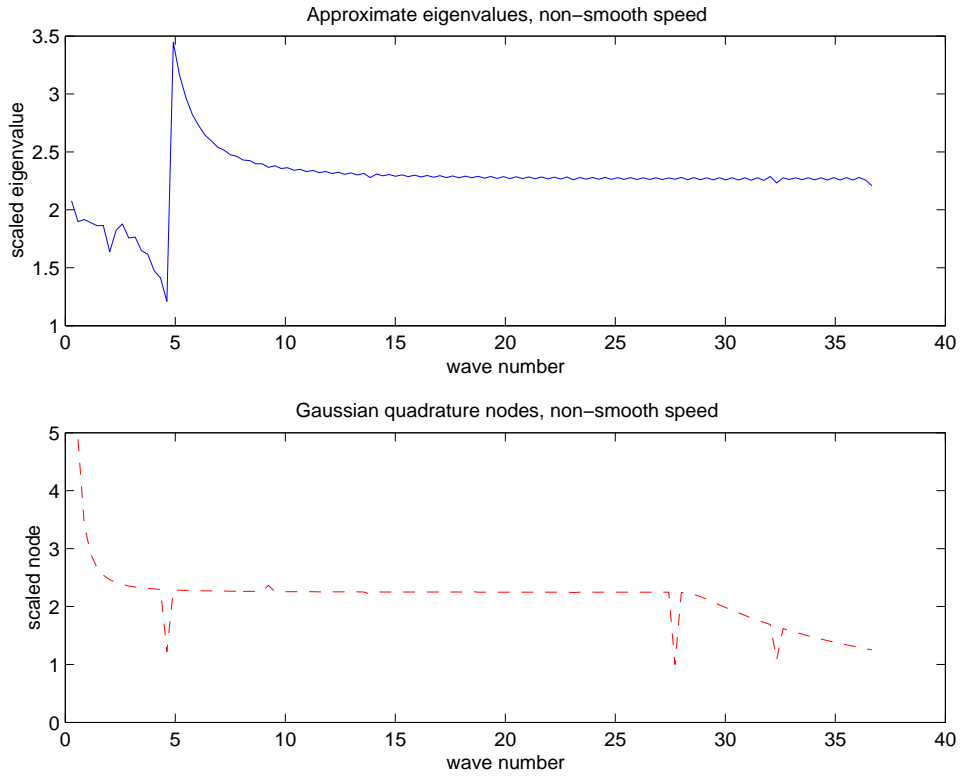


Figure 12: Approximate eigenvalues of the operator $\mathcal{A} = (1 + \frac{1}{2} \cos(32\pi x)) \partial_{xx}$, and Gaussian quadratures nodes of a 2-point rule used to approximate $\langle \phi_\omega, f(\tilde{\mathcal{A}}) \phi_\omega \rangle$ where $\tilde{\mathcal{A}}$ is defined in (3.7), plotted against the wave number ω . For each eigenvalue, the wave number is determined by the dominant frequency of the corresponding approximate eigenfunction.